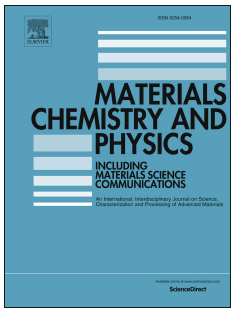
Journal Pre-proof



PAN/CA-based electrospun membranes for air filtration and active microorganism degradation

Joana M. Rocha, Rui P.C.L. Sousa, Joana C. Araújo, Sofia M. Costa, Wilson Antunes, Verónica Rocha, Raul Fangueiro, Diana P. Ferreira

PII: S0254-0584(25)01507-X

DOI: https://doi.org/10.1016/j.matchemphys.2025.131861

Reference: MAC 131861

To appear in: *Materials Chemistry and Physics*

Received Date: 30 July 2025

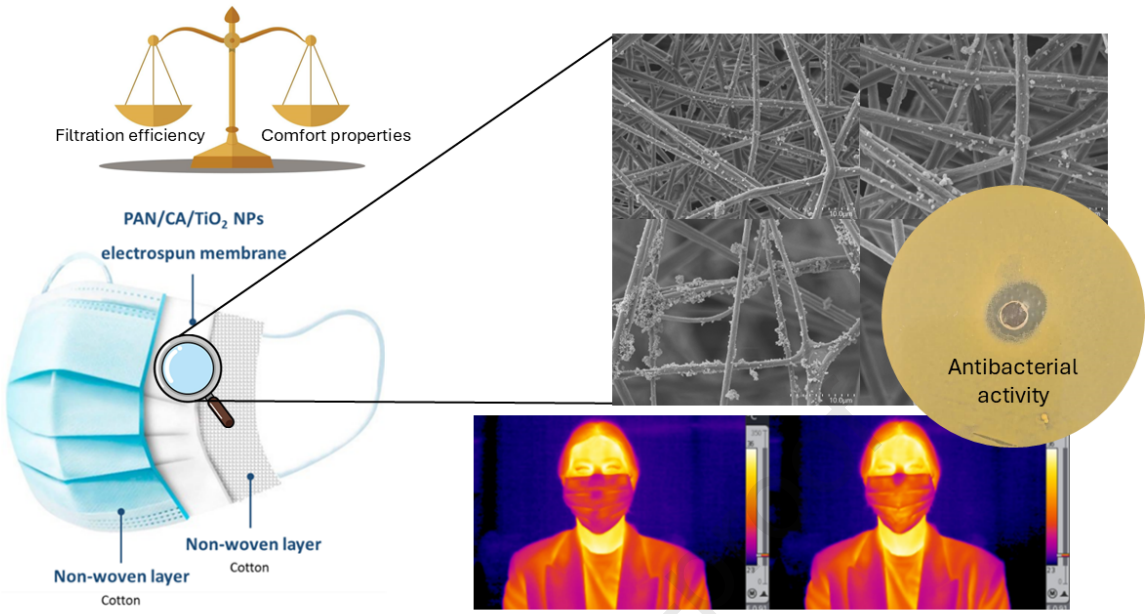
Revised Date: 3 October 2025

Accepted Date: 26 November 2025

Please cite this article as: J.M. Rocha, R.P.C.L. Sousa, J.C. Araújo, S.M. Costa, W. Antunes, V. Rocha, R. Fangueiro, D.P. Ferreira, PAN/CA-based electrospun membranes for air filtration and active microorganism degradation, *Materials Chemistry and Physics*, https://doi.org/10.1016/j.matchemphys.2025.131861.

This is a PDF of an article that has undergone enhancements after acceptance, such as the addition of a cover page and metadata, and formatting for readability. This version will undergo additional copyediting, typesetting and review before it is published in its final form. As such, this version is no longer the Accepted Manuscript, but it is not yet the definitive Version of Record; we are providing this early version to give early visibility of the article. Please note that Elsevier's sharing policy for the Published Journal Article applies to this version, see: https://www.elsevier.com/about/policies-and-standards/sharing#4-published-journal-article. Please also note that, during the production process, errors may be discovered which could affect the content, and all legal disclaimers that apply to the journal pertain.

© 2025 Published by Elsevier B.V.



Journal Pre-proof

Journal Pre-proof

PAN/CA-based electrospun membranes for air filtration and active microorganism degradation

Joana M. Rocha [1], Rui P. C. L. Sousa [1,*], Joana C. Araújo [1], Sofia M. Costa [1], Wilson Antunes [2], Verónica Rocha [1], Raul Fangueiro [1], and Diana P. Ferreira [1,*]

[1] Centre for Textile Science and Technology (2C2T), University of Minho, 4800-056 Guimarães, Portugal

[2] Centro de Investigação da Academia Militar (CINAMIL), Unidade Militar Laboratorial de Defesa Biológica e Química (UMLDBQ, Instituto Universitário Militar), Av. Dr. Alfredo Bensaúde, 1849-012 Lisboa, Portugal

Correspondence: rui.sousa@2c2t.uminho.pt; diana.ferreira@det.uminho.pt

Abstract

Designed to efficiently remove particulates and degrade microorganisms, active filtration membranes enhance filtration efficiency while minimizing pressure drop and maintaining airflow. The COVID-19 pandemic has heightened demand for high-efficiency facemasks, driving the pursuit of new materials with enhanced filtration, multifunctionality, and biodegradability. Among fabrication methods, electrospinning stands out as a versatile and cost-effective technique for producing fibrous membranes with high surface-to-volume ratio, porosity, and tuneable properties.

Herein, we report the development of electrospun membranes for active filtration functionalized with titanium dioxide (TiO_2) nanoparticles (NPs) to be used as intermediate layers for facemasks. This research investigates the use of polyacrylonitrile (PAN) and cellulose acetate (CA) for fibrous membrane fabrication, combining PAN's chemical stability and CA's biocompatibility. TiO_2 NPs were synthesized and characterized to functionalize the produced membranes by electrospraying, after the confirmation of the antibacterial activity of the NPs. The functionalized membranes were characterized through morphological, chemical, thermal, and mechanical analyses. Besides, the porosity and filtration efficiency of the functionalized membranes were also evaluated. PAN/CA/TiO_2 NPs membranes showed filtration efficiencies above 80% for 1 µm particles, showcasing their effectiveness in particulate removal. Facemask prototypes were fabricated by integrating the PAN/CA/TiO_2 NPs membranes between two layers of cotton woven fabric. The prototypes were tested for air permeability and thermal comfort, showing significant potential for practical applications.

Journal Pre-proof

Keywords: polyacrylonitrile; cellulose acetate; titanium dioxide nanoparticles; filtration; facemask

1. Introduction

Air filtration membranes with active filtration are made to effectively filter out germs, aerosols, and particles. These membranes are essential for preserving indoor air quality and safeguarding public health [1]. The ability of active filtration membranes to actively degrade microorganisms while preserving other filtration membrane properties like filtration efficiency, low pressure drop, and air flow penetration during the filtering process is what makes them so important [2,3]. These membranes can achieve high filtration effectiveness while maintaining high air permeability by using novel materials and structures, like electrospun nanofibers, which helps to effectively purify the air [4,5].

Overall, active filtration membranes play a crucial role in various applications ranging from air and water filtration to multi-layer protective systems. In recent years, the development of facemasks with high filtration efficacy and the capacity to degrade microorganisms has become a widely studied field, primarily as a result of the high demand for these materials that has been induced by the COVID-19 pandemic [6]. This is especially important in the post-pandemic context, as active degradation of pathogens helps reduce the risk of recontamination and cross-infection during repeated handling and prolonged mask use. The development of materials with enhanced biodegradability, multifunctionality, and filtration efficiency is becoming more and more important. Additionally, preventing bacteria from building up and penetrating through the mask requires active destruction [5,7,8].

Electrospinning is one of the most used techniques to manufacture active layers of nanofibers for facemask applications. Its versatility, wide range of spinnable materials, and good cost-effectiveness ratio make it a promising technique for a large array of applications [9]. Electrospun membranes are highly desirable for the development of high-performance filters due to their small diameters, ranging from nanometers to micrometers, high surface-to-volume ratio, high porosity, ease of surface functionalization, and high flexibility in adjusting their size and shape [10]. Owing to their high permeability and minimal weight, these fibrous membranes offer superior filtration efficacy while preserving the wearer's comfort and breathability [11,12].

Journal Pre-proof

Adding to the advantages of electrospun membranes, filtration performance is greatly influenced by the polymer selection. To date, the electrospinning method has been used to create air filtration membranes using a variety of polymers. Polyacrylonitrile (PAN) is a synthetic polymer commonly used in the production of electrospun membranes due to its mechanical, thermal, and chemical stability. Several electrospun PAN nanofibrous membranes have shown excellent air-dust filtration effectiveness, surpassing over 99.99% efficiency for particles ranging from $PM_{0.3}$ to $PM_{2.5}$ (Particulate Matter). Additionally, PAN nanofiber membranes have shown high water permeability, making them versatile for various filtration applications [13]. Cellulose acetate (CA) is a natural polymer with high interest due to its biocompatibility, biodegradability, and mechanical reinforcement properties [14]. Because of their special qualities, which include high air permeability and appropriateness for air filtration applications, especially in capturing aerosols and volatile organic compounds (VOCs), CA membranes have been employed in air filtration [15]. The combination of these two polymers can join promising properties for the development of filtration layers. While both PAN and CA have been individually explored in electrospun membranes, combining them into a single formulation allows for synergistic benefits by leveraging PAN's mechanical stability and filtration efficiency alongside CA's biocompatibility and biodegradability [16–18]. This combination may facilitate more effective interaction with microorganisms, enhancing active degradation and broadening their potential for practical facemask applications.

The functionalization of electrospun membranes with metal oxide nanoparticles (NPs) is an excellent strategy to achieve an active filter layer. NPs can give these materials new capabilities including the breakdown of chemical and biologically hazardous substances because of their unique properties, nanoscale size, and high surface area-to-volume ratio. [19]. Studies have shown that incorporating titanium dioxide (TiO_2) NPs into membranes can enhance their properties, especially air filtration performance [20–22]. Furthermore, the addition of TiO_2 NPs has been preferred due to its multifunctional properties, including thermal and physical resistance, antibacterial and photocatalytic activity, which are beneficial for filtration purposes [23–25]. Among the possible functionalization methodologies, electrospraying stands out for its ability to deposit nanoparticles directly onto the fiber surface [26,27]. The nanoparticles'

Journal Pre-proof

surface localization is especially beneficial since it guarantees a more direct interface between the NPs and the environment, improving the membrane's photocatalytic and antibacterial efficacy without substantially changing its internal structure [22,28,29].

Therefore, the main objective of this work was to develop PAN/CA electrospun membranes functionalized with TiO_2 NPs for active filtration to be used as intermediate layers for facemasks. To the best of the authors' knowledge, this is the first study reporting the development of PAN/CA electrospun membranes, functionalized with TiO_2 NPs, integrated into real facemask prototypes. While previous works have focused on material characterization, the novelty of this work includes the demonstration of the practical feasibility of the material, included on ready-to-use facemask prototypes that were characterized in terms of comfort properties.

The first part of this work focused on the development and optimization of defect-free and uniform PAN/CA electrospun membranes. PAN and PAN/CA electrospun membranes were characterized by Scanning Electron Microscopy (SEM), Attenuated Total Reflectance-Fourier Transform Infrared Spectroscopy (ATR-FTIR), Thermogravimetric Analysis (TGA), and mechanical assays, to investigate the influence of CA incorporation. TiO_2 NPs were synthesized and characterized by Scanning Transmission Electron Microscopy (STEM), ATR-FTIR and antibacterial tests.

Electrospraying was performed to functionalize the membranes with TiO_2 NPs. Characterization of all the functionalized membranes was carried out by Ground State Diffuse Reflectance (GSDR), SEM, Energy Dispersive Spectroscopy (EDS), and Water Contact Angle (WCA), to study the suitability of the functionalization. The porosity and the filtration efficiency of the membrane were also evaluated. In the end, the PAN/CA/TiO_2 NPs membranes were used for developing facemask prototypes, with cotton natural fiber serving as outer layers. The developed facemask prototypes were evaluated in terms of air permeability and thermal comfort.

2. Materials and Methods

2.1. Materials

Polyacrylonitrile (PAN), M_w=150.000 g/mol, was purchased from Sigma-Aldrich, and Cellulose Acetate (CA), M_w=100.000 g/mol, from Thermo Scientific. Dimethylformamide

(DMF) and Ethanol were obtained from Fisher Chemical. Titanium Butoxide (IV) was acquired from Sigma-Aldrich. All reagents and solvents were used as received.

2.2. Electrospun PAN and PAN/CA membranes

2.2.1. Preparation of PAN and PAN/CA solutions

PAN solutions with a total concentration of 10 % (w/v) were prepared by gradually adding PAN pellets to a DMF solution at room temperature [30]. The solution was kept under mechanical stirring until a homogeneous appearance was achieved. For PAN/CA solutions, a CA concentration of 1 % (w/v)) was added gradually to the previously prepared PAN polymeric solution. The final formulations were stored until further use in the electrospinning process.

2.2.2. Optimization of the electrospinning process

All solutions were electrospun using a MECC NF-103 electrospinning equipment. The polymer solution was introduced in a 24 mL syringe with a 0.61 mm diameter needle. A static collector was used to collect the electrospun membranes. Humidity and temperature values were kept stable at 50-60 % and 19-25 °C, respectively. The optimized processing conditions that allowed stable jet formation and defect-free nanofiber production are shown in Table 1.

Table 1: Optimized electrospinning process parameters to produce PAN and PAN/CA membranes.

Parameters	Optimized values
Voltage	30 kV
Flow rate	0.5 mL/h
Needle-collector distance	150 mm
Needle diameter	0.61 mm
Deposition time	4 h
Head Transverse Speed	50 mm/s
Head Transverse Distance	150 rpm

2.3. Functionalization of PAN/CA electrospun membranes with TiO_2 NPs

2.3.1. Synthesis of the TiO_2 NPs

The synthesis of TiO_2 NPs was performed as previously reported [31], by the gradual addition of $Ti(OBu)_4$ to distilled water. The solution was kept under mechanical stirring at 40 °C for 30 min. The precipitate was centrifuged, washed with water and ethanol,dried for 2 days at room temperature, and then calcinated at 150 °C for 6h.

Journal Pre-proof

2.3.2. Functionalization of TiO_2 NPs into PAN/CA electrospun membranes

After the development of PAN/CA membranes by electrospinning, the produced membranes were functionalized with the TiO_2 NPs by electrospraying. Briefly, an ethanolic solution of TiO_2 NPs (3 % w/v) was used for electrospraying the previously produced PAN/CA electrospun membranes on both sides of the membrane. The solution of TiO_2 NPs was transferred into a 24 mL syringe coupled to a needle with a diameter of 0.41 mm. Humidity and temperature values were kept stable at 50-60 % and 19-25 °C, respectively. The final processing conditions used for the electrospraying of the TiO_2 NPs are shown in Table 2.

Table 2: Electrospraying parameters for deposition of TiO_2 nanoparticles onto PAN/CA membranes.

Parameters	Optimized values
Voltage	29 kV
Flow rate	1 mL/h
Needle-collector distance	300 mm
Needle diameter	0.41 mm
Deposition time	2 h
Head Transverse Speed	50 mm/s
Head Transverse Distance	150 rpm

2.4. Sample characterization

2.4.1. Scanning Transmission Electron Microscopy (STEM)

Using a NOVA 200 Nano SEM from FEI Company (Hillsboro, OR, USA) with a scanning transmitted electron microscopy detector, the morphology of the synthetized NPs was studied by STEM. An ethanol suspension of the TiO_2 NPs was used to dip the STEM grids used for the morphological characterization. The grids were then dried and used to assess the morphology of the NPs.

2.4.2. Scanning Electron Microscopy (SEM) and Energy Dispersive Spectroscopy (EDS)

A FlexSEM 1000 II (HITACHI) was used to assess the morphology of the electrospun membranes by SEM. With a Quorum MiniQS sputter coater, a thin layer of gold (Au) was applied on the surface of each sample. A 5 kV acceleration voltage was used to capture secondary electron pictures. A coupled Bruker energy dispersive X-ray detector (EDS) was used to assess the percentages of each atom.

Journal Pre-proof

2.4.3. Attenuated Total Reflectance-Fourier Transform Infrared Spectroscopy (ATR-FTIR)

An IRAffinity-1S apparatus, SHIMADZU (Kyoto, Japan), fitted with an ATR accessory, was used to analyze the chosen materials using ATR-FTIR spectroscopy. Each spectra was obtained in the 400–4000 cm^{-1} region using transmittance mode in a diamond ATR cell by accumulating 45 scan cycles with a resolution of 4 cm^{-1}. To guarantee the homogeneity of the analysis, several samples were examined at various sites.

2.4.4. Ground-State Diffuse Reflectance (GSDR)

The produced electrospun membranes were analyzed by GDSR, using a Spectrophotometer UV-2600 (Shimadzu) equipped with an ISR_2600 Plus detector to record the transmittance and reflectance spectra. The equipment was calibrated using barium sulfate as reference (full reflectance). To guarantee the homogeneity of the analysis, the samples were analyzed at various points. The reflectance spectra were recorded in the 200 to 800 nm wavelength, and the remission function was calculated accordingly with the Kubelka–Munk equation:

$$\frac{K}{S} = \frac{[(1 - R)]^2}{2 \times R} \quad (1)$$

Where K represents the absorption coefficient, S represents the dispersion coefficient, and R represents the reflectance.

2.4.5. Thermogravimetric analysis (TGA)

Using TGA, the thermal stability of the membranes was verified. The primary objective of this technique is to monitor the mass loss of a sample as a function of temperature increase in the presence of a controlled atmosphere [32]. The thermal behavior of the produced membranes was examined using STA 7200 SCANSCI apparatus. Over a temperature range of 25 to 1000 °C, the TGA curve was generated in a nitrogen environment at a steady heating rate of 10 °C/min. The samples were put in a crucible that was attached to a microbalance in order to conduct the analysis. The crucible was then heated under controlled conditions, and the mass losses were monitored.

Journal Pre-proof

2.4.6. Mechanical tests

Tensile experiments were carried out to assess the mechanical characteristics of the produced membranes. A Hounsfield Tinius Olsen, model H100KS, fitted with a 250 N load cell and an HT400 Pneumatic Grip Controller, was used for these testing. The samples were cut into strips with 70 mm length and 30 mm width. The crosshead speed was set at 10 mm/min, and the initial grip separation was set at 50 mm. The ASTM 5035 Norm was followed. From the stress-strain curves, the tensile strength, elongation at break, and Young's modulus were determined. For every sample, three replicates were examined. The calculations for stress (σ), strain (ε) and Young's modulus (E) followed equations 2 to 4.

$$\sigma = \frac{F}{A} \quad (2)$$

$$\varepsilon = \frac{\Delta L}{L_0} \quad (3)$$

$$E = \frac{\Delta \sigma}{\Delta \varepsilon} \quad (4)$$

Where F represents the applied force (N), A is the initial cross-sectional area of the sample (mm^2), ΔL is the change in length (mm) and L_0 is the initial sample length (mm). Δσ and Δε correspond to the variations in stress and strain within the elastic deformation range.

2.4.7. Water Contact Angle Measurement (WCA)

WCA was used to evaluate the hydrophobicity of the different electrospun membranes, using a Contact Angle System (dataphysics) coupled to a high-resolution camera. 5 µL of distilled water was dispensed onto the sample's surface using a syringe. Ten different places of each sample were measured, to guarantee the homogeneity of the analysis, and the mean and the standard deviation values were calculated.

2.4.8. Evaluation of Antibacterial Activity

Antibacterial activity of the TiO_2 NPs was tested against both Gram-positive bacteria, *Staphylococcus aureus* (ATCC 6538), and Gram-negative bacteria, *Escherichia coli* (ATCC 25922). Tryptic soy broth (TSB) medium was used for the cultivation of freshly growing bacteria. Each bacterium grew overnight at 37 °C, then the cell suspension was adjusted

Journal Pre-proof

to a final concentration of approximately 1×10^7 bacteria/mL. Using sterilized cotton swabs, 100 µL of each cell suspension was spread on a Tryptic soy agar (TSA). Subsequently, the agar medium was punched with 6 mm diameter wells and filled with 50 µL of 1% TiO_2 NPs and the plates were maintained at 37 °C for 24 h. The antibacterial activity was determined by measuring the diameter of the growth inhibition zone (or halo), in mm. Each test was performed in duplicate.

2.4.9. Porosity analysis

The porosity analysis was performed on a capillary flow gas-liquid porometer with patented pressure step stability POROLUX™ Revo. The membrane was analyzed using as wetting liquid Porefil (16.0 dyn/cm) and a shape factor of 1. Before the measurement, the disc of Ø = 13 mm diameter was cut from the membrane sheet. The sample disc was then placed into the instrument and wetted with Porefil directly within the sample holder to prevent wrinkling. A wet run was performed, followed by a dry run to obtain the flow rate curves as a function of applied pressure. The measurements were carried out in triplicate to enhance the reliability of the results.

2.4.10. Filtration assays

The filtration tests were performed in a cylindrical acrylic chamber (Ø = 194 mm × length = 400 mm) developed for the controlled release of particles and mounted inside a 1 m^3 negative pressure flexible isolator (Solocontainment™, Cheshire, UK). Polystyrene beads (Ø = 1 µm, COUNT-CAL™ Count Precision Size Standards Thermo Fisher) were aerosolized using a medical nebulizer (OMRON C28P) with a flow rate of 0.5 mL/min to obtain a final number of particles between 1×10^6 and 4×10^6 inside the aerosolization compartment of the acrylic chamber. The number of particles were measured in real time using a laser particle counter (APEX R4 airborne particle counter, LighthouseTM, Fremont, CA, USA) installed above the aerosolization compartment of the chamber. The testing membranes were mounted in a leak tight sample port positioned above the aerosolization compartment and inside the counting compartment of the acrylic chamber, where the inlet of the laser particle counter was installed. Polystyrene particles released inside the aerosolization compartment were aspirated through the sample port at a rate of 28.2 L/min and measured three times during 20 s

for a total of 60 s. The acrylic chamber was cleaned between tests using a HEPA vacuum cleaner (KARCHERTM A2204, Winnenden, Germany), and the cutoff value to consider the chamber clean for tests was below 4000 particles. The residual number of particles inside the acrylic chamber were counted through a blank measurement between cleaning procedures and sample loading.

2.5. Prototype development

Different facemask prototypes were developed using two layers of cotton woven fabric and the selected PAN/CA/TiO_2 NPs electrospun membrane, namely: (i) Cotton + Cotton; (ii) Cotton + PAN/CA/TiO_2 NPs electrospun membrane + Cotton and (iii) Cotton + 2 × PAN/CA/TiO_2 NPs electrospun membrane + Cotton.

2.5.1. Air Permeability

The FX3300 Air Permeability Tester III (TexTest instrument, WanJiang, Dongguan, China) was used to measure the rate of airflow through a 20 cm^2 area passage at a pressure of 200 Pa for one minute to determine the air permeability of the electrospun membranes and the facemask prototypes. The air permeability, k, was calculated accordingly with the equation 5 [33]:

$$k = \frac{(\frac{L}{m^2 s}) \times t \times A}{1000} \quad (5)$$

Where $(\frac{L}{m^2 s})$ represents the rate of air flow, t represents the time in seconds, and A represents the sample area.

2.5.2. Thermal Management

A Thermal Imaging Camera Testo 885 was used to assess the thermal comfort of the different facemask prototypes. Two conditions, namely during inhalation and exhalation, were assessed. Following a period of early stabilization, temperature variations in the nose and mouth were measured using thermal imaging. The camera's temperature range was specified as 20–40 °C.

Journal Pre-proof

3. Results and discussion

3.1. Electrospun PAN and PAN/CA Membranes

This work focused on the development of active filtration electrospun membranes based on PAN due to its high chemical resistance and filtration efficiency. A 10% (w/v) PAN solution in DMF was electrospun to produce a defect-free membrane, using optimized parameters: a 150 mm needle-to-collector distance, 0.5 mL/h flow rate, 30 kV applied voltage, and a deposition time of 4 hours. CA was added to the optimized PAN formulation (1 % (w/v)) [34]. To assess the effect of the CA addition on the morphology, chemical, and mechanical properties of the produced fibers, the conditions of the electrospinning process were kept the same as those used on PAN deposition. The developed electrospun PAN and PAN/CA membranes were characterized by SEM, ATR-FTIR and tensile tests.

SEM analysis was performed to evaluate the surface morphology and diameters of the developed electrospun fibers. Figure 1 shows the SEM images of the fibers produced by electrospinning using PAN and PAN/CA, as well as the corresponding frequency distribution of fiber diameter. As can be seen, defect-free PAN and PAN/CA fibers were successfully produced. SEM characterization of the PAN membranes revealed diameters of the produced fibers between 0.6 and 1.3 µm (Figure 1a). It can be seen that the addition of CA slightly increased the diameter of the fibers, from an average value of 0.869 µm to an average value of 1.21 µm, as previously reported in the literature (Figure 1b) [35]. Moreover, the addition of CA resulted in a more homogeneous distribution of the fibers.

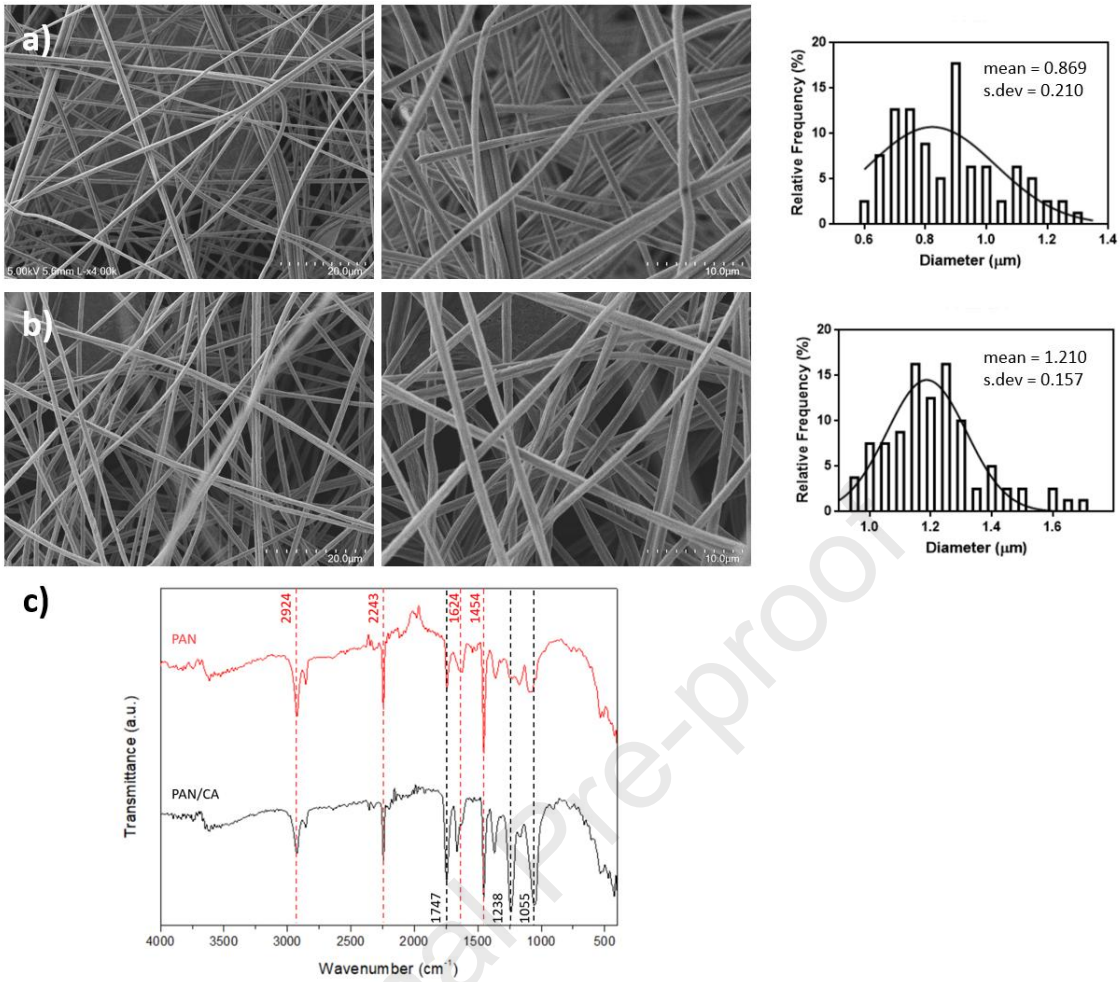


Figure 1: Morphological and chemical characterization of electrospun membranes: (a) SEM analysis of PAN fibers at 20 and 10 μm and respective fiber diameter distribution histograms; (b) SEM analysis of PAN/CA fibers at 20 and 10 μm and respective fiber diameter distribution histograms; (c) ATR-FTIR spectra of PAN and PAN/CA membranes.

ATR-FTIR analysis was performed to confirm the chemical composition of PAN and PAN/CA electrospun membranes. Figure 1c shows the ATR-FTIR spectra for the two membranes. The spectrum of the PAN membranes reveals the characteristic bands of this polymer. The sharp peaks at 2924 cm^{-1} and 2243 cm^{-1} correspond to C-H stretching and nitrile group stretching (C≡N), respectively. A weak peak at 1624 cm^{-1} is related to C≡N, 1454 cm^{-1} is related to C-H bending, while 1362 and 1242 cm^{-1} are related to aliphatic CH groups (CH, CH_2, CH_3) [36,37]. Comparison with the PAN/CA spectrum shows the presence of CA with the appearance of polymer's characteristic sharp peaks at 1238 (C-O stretching) and 1747 cm^{-1} (C=O stretching) [38]. Additionally, the reduced intensity of the nitrile peak at 2243 cm^{-1} supports the presence of intermolecular interactions—such as hydrogen bonding—between PAN and CA, highlighting a key

difference from previous studies where no chemical interaction between the two polymers was reported [35].

Tensile tests were also conducted to analyze the different mechanical properties of PAN and PAN/CA membranes. Table 3 shows the values of tensile strength, maximum stress deformation, breaking point, strain, and Young's modulus. The PAN sample exhibits a tensile strength of 0.208 MPa and a maximum strain of 11.2 %, while the PAN/CA sample demonstrates a significantly higher tensile strength of 0.599 MPa and a maximum strain of 14.4%. These improvements are particularly relevant for membrane applications, as higher tensile strength indicates a greater ability of the material to withstand applied forces without breaking, which is essential for structural integrity during operation. Similarly, the increase in maximum strain suggests that the PAN/CA membrane can sustain larger deformations before failure, contributing to greater durability and flexibility under mechanical stress. In practical terms, this means the membrane is less likely to rupture or degrade when subjected to physical handling or pressure differentials during use. Furthermore, Young's Modulus indicates a higher stiffness for PAN/CA (20.66×10^{-5} GPa) compared to PAN (5.77×10^{-5} GPa), showing a 358% increase. A previous study showed that PAN/CA electrospun membranes with a CA content higher than 50% showed lower tensile strength and Young's moduli when compared with pure PAN membrane [35]. However, this study showed that lower CA content was able to improve both strength and stiffness of pure PAN. The results herein reported suggest that 10% PAN / 1% CA membrane generally has better mechanical performance compared to the PAN membrane, particularly in terms of strength and stiffness, indicating that the addition of a smaller amount of CA improved the mechanical properties of the produced PAN structures.

Table 3: Mechanical properties of electrospun PAN and PAN/CA membranes, including tensile strength, elongation at break, and Young's modulus.

Sample	Tensile Strength (MPa)	Maximum Strain (%)	Young's Modulus (GPa)	R^2
PAN membrane	0.208 ± 0.087	11.2 ± 4.4	$(5.77 \pm 2.39) \times 10^{-5}$	0.976 ± 0.037
PAN/CA membrane	0.599 ± 0.068	14.4 ± 2.5	$(20.66 \pm 7.65) \times 10^{-5}$	0.991 ± 0.008

Overall, the incorporation of CA into the PAN matrix significantly improves the membrane's mechanical properties and promotes a more homogeneous fiber

distribution, making it better suited for applications that demand greater strength, flexibility, and structural reliability.

3.2. Functionalization of PAN/CA electrospun membranes with TiO2 NPs

The synthesis of TiO_2 NPs was performed by a straightforward, sustainable precipitation method previously reported by the group [31]. The synthesized TiO_2 NPs were analyzed by STEM and ATR-FTIR to confirm their morphology and purity. STEM characterization (Figure 2a and 2b) shows that the produced NPs present a spherical morphology. The formation of agglomerates, commonly observed for this type of nanoparticle, is consistent with findings reported in the literature [39]. The mean calculated diameter was found to be 43 nm, similar to previous reports [31]. ATR-FTIR analysis (Figure 2c) was also performed for the synthesized TiO_2 NPs. The spectrum shows the characteristic Ti-O stretching vibration band at around 400 cm^{-1}, considered the fingerprint region for TiO_2, therefore confirming the purity of the NPs [40]. Overall, the synthesized TiO_2 NPs exhibited the expected morphological and chemical characteristics, confirming that they were successfully and reliably produced with high quality.

The synthesized TiO_2 NPs were also evaluated for their antibacterial activity to assess their potential to functionalize PAN/CA electrospun membranes into active filtration membranes, with the ability to degrade/inactivate microorganisms. The antibacterial properties of TiO_2 NPs activity have been widely reported, due to the generation of reactive oxygen species (ROS), which induce oxidative stress leading to cell membrane damage and microbial death [31,41,42]. In this study, the NPs were analyzed by the zone of inhibition test, revealing a halo of 15-15.5 mm in the presence of the Gram-positive bacteria *Staphylococcus aureus*, as shown in Figure 2d. This finding demonstrates the antibacterial activity of the synthesized TiO_2 NPs against *S. aureus* bacteria.

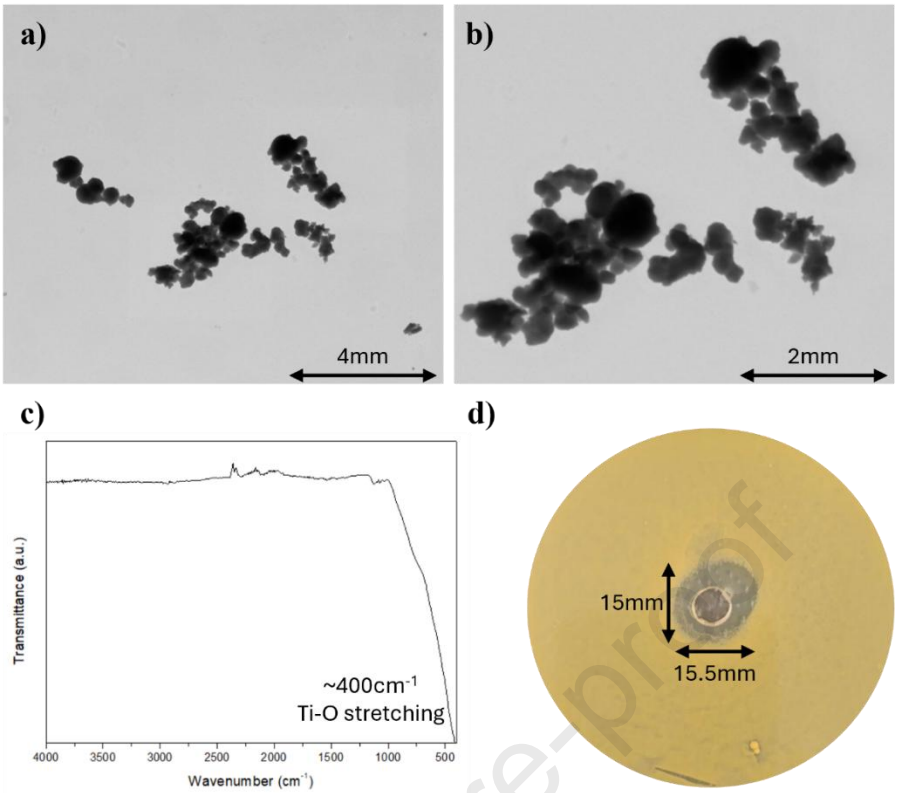


Figure 2: Characterization of synthesized TiO_2 nanoparticles: (a, b) STEM images at 25,000× and 50,000× magnification; (c) ATR-FTIR spectrum; (d) Zone of inhibition test against *S. aureus.*

The functionalization of the PAN/CA electrospun membrane with TiO_2 NPs was performed via electrospraying, ensuring their availability on the membrane surface to serve as an active filtration layer, unlike previous studies reported in the literature [18]. An ethanolic solution of TiO_2 NPs (3% w/v) was electrosprayed on both sides of the previously developed PAN/CA membrane. Electrospraying conditions were optimized, and the ideal conditions were found to be as described in Table 2. PAN/CA/TiO_2 NPs membrane was then characterized to assess the suitability of the functionalization method and the functional properties of the membrane for active filtration applications.

3.3. Characterization of PAN/CA/TiO_2 NPs electrospun membranes

The PAN/CA electrospun membranes functionalized with TiO_2 NPs were characterized to assess whether the functionalization was successful. ATR-FTIR analysis was not conclusive for confirming the integration of TiO_2 NPs into the membrane, as the characteristic Ti–O stretching bands (400–500 cm^{-1}) overlap with the absorption bands of PAN in the same spectral region (Figure S1).

Therefore, Ground-State Diffuse Reflectance was used to assess the functionalization success. Figure 3a shows the GSDR spectra of PAN/CA and PAN/CA/TiO_2 NPs electrospun membranes. It is possible to observe that the spectrum of PAN/CA shows a clean spectrum between 250 and 800 nm. On the other hand, PAN/CA/TiO_2 NPs spectra reveals the appearance of a broad absorption band at around 300 nm, characteristic of TiO_2 NPs [43].

This was confirmed by the SEM/EDS analysis, in which it was possible to detect the presence of TiO_2 NPs in the surface of PAN/CA membrane. Figure 3b represents SEM images PAN/CA/TiO_2 NPs membrane, as well as the EDS graph revealing the titanium and oxygen percentage. SEM images reveal the presence and the homogeneous distribution of TiO_2 NPs in the fibers surface, as well as their attachment to the PAN/CA electrospun membranes. EDS analysis reveals the presence of a strong peak at around 4.5 keV, related to the presence of titanium, besides carbon and oxygen peaks from the PAN/CA membrane and gold peaks from the coating. The percentage of titanium was measured in different places and was found to be 2.89 ± 0.24 %.

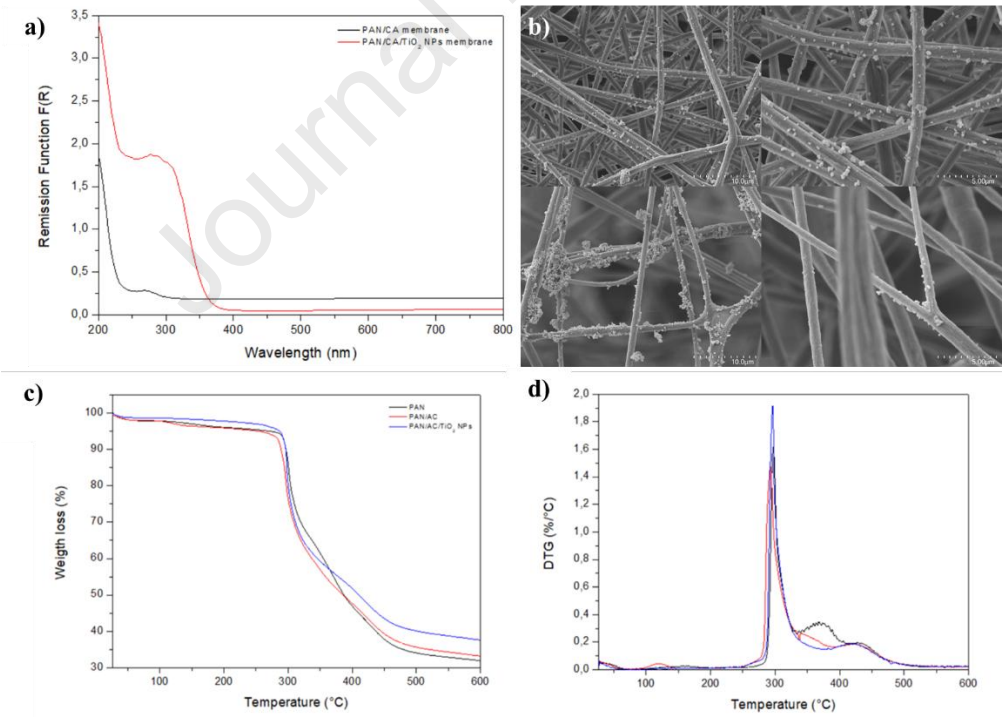


Figure 3: Characterization of functionalized PAN/CA membranes: (a) GSDR spectra of PAN/CA and PAN/CA/TiO_2 NPs; (b) SEM analysis of PAN/CA/TiO_2 NPs; (c) TGA spectra of PAN, PAN/CA, and PAN/CA/TiO_2 NPs; (d) DTG curve for of PAN, PAN/CA, and PAN/CA/TiO_2 NPs.

TGA was performed to evaluate the thermal stability and degradation behavior

of PAN, blended PAN/CA membranes, and PAN/CA/TiO_2 NPs membranes. Figure 3c reveals the TGA and DTG curves for the 3 membranes. All the samples show small mass losses between 80 and 120 °C, as a result of residual solvent evaporation. Regarding the main degradation processes, these are shown between 290 and 450 °C.

For the pristine PAN membrane, the main degradation occurs in a sharp temperature range between 290 and 310 °C which is related to the nanofibers' pyrolysis and breakdown of nitrile groups, typical of PAN [44]. Smaller degradation processes are seen up until 450 °C. Specifically, a secondary major degradation process is visible in the DTG curve of PAN between 350 and 400 °C, which can be associated with late-stage degradation and cyclization products of PAN [45]. The addition of CA to the polymer solution did not have a significant impact on the thermal properties, since the degradation of CA normally occurs between 320 and 350 °C [46]. Nevertheless, a broadening of the main degradation peak can be observed, and the weakening of the peak between 350 and 400 °C suggests that the presence of CA dilutes or modifies the PAN network formation, thereby suppressing late-stage PAN degradation. This further confirms the findings from the FTIR analysis, which indicated the presence of intermolecular interactions between PAN and CA.

The functionalization with TiO_2 NPs does not significantly change the thermal decomposition behavior of the PAN/CA membrane. The PAN/CA/TiO_2 NPs membrane retains a higher mass percentage at 600 °C, as evidenced by its increased char yield of 37.48 %, compared to 33.20 % for PAN/CA. Considering that the TiO_2 NPs have residues of 100 % at 600 °C, the TGA analysis allows to estimate the percentage of TiO_2 NPs in the PAN/CA membrane, by using Equation 1. This value was found to be approximately 6.41 %, confirming the successful deposition of the NPs into the membrane's surface.

In order to study the hydrophobicity of the developed membranes', the WCA was evaluated. This parameter is particularly important, since filtration layers shall be hydrophobic to avoid the presence of virus droplets inside the layer [47]. The results obtained are exhibited in Table 4. A surface is classified as hydrophilic if its WCA value is less than 90° and hydrophobic if it is greater than 90°. If the WCA is greater than 150°, the surface could be regarded as superhydrophobic [48]. Analysis of the contact angle with water showed that the produced PAN-based membranes, with and without CA, are

Journal Pre-proof

hydrophobic. PAN's known hydrophobicity is explained by its strong chain crystallinity, resulting in limited water penetration [49]. penetrate or hydrogen-bond with the tightly packed PAN chains. The addition of the CA didn't change the contact angle of the membranes, keeping their repellency. The acetyl groups make CA more hydrophobic than pure cellulose and the small percentage of CA used allows for maintaining the hydrophobicity of the membrane. Furthermore, the introduction of TiO_2 NPs also does not affect the hydrophobic character of PAN/CA membranes. Although TiO_2 can show hydrophilic behaviour due to the formation of surface hydroxyl groups that increase its surface energy and can hydrogen-bond with water [50], TiO_2 NPs often exhibit hydrophobic behavior because, in aggregated form, they create micro/nanoscale roughness on the membrane surface that amplifies hydrophobicity through the Cassie-Baxter effect [51]. As a result, their presence in small amounts does not significantly increase the membrane's surface energy or introduce hydrophilic groups capable of lowering the water contact angle [52].

Table 4: Water contact angle measurements of PAN, PAN/CA, and PAN/CA/TiO_2 NPs electrospun membranes.

Sample	Water Contact Angle	Classification
PAN	132 ± 4 °	Hydrophobic
PAN/CA	131 ± 4 °	
PAN/CA/TiO_2 NPs	128 ± 14 °	

The porosity of the PAN/CA/TiO_2 NPs electrospun membrane was analyzed by capillary flow porometry. Table 5 shows the bubble point pore size, the mean flow pore (MFP) size, the smallest pore size, and the total pore area of the functionalized membrane. The MFP size was found to be 11.09 µm, indicating the presence of macropores that contribute to fast air and fluid flow, which is advantageous for applications in filtration and breathability. Moreover, a bubble point pore size of 15.53 µm and a smallest pore size of 10.56 µm suggest a relatively narrow pore size distribution, which is desirable for maintaining selectivity while preserving permeability. Furthermore, the pore size values fall within the ideal range for particulate filtration (0.1–20 µm), aligning with previous findings where PAN-based electrospun membranes have been tailored for fine dust and pathogen filtration [41,53]. The total pore area of 54.71% confirms that the membrane possesses a highly porous structure. Porosity

Journal Pre-proof

values above 50% are typically associated with effective air permeability and low-pressure drops, critical parameters for membranes intended for respiratory or environmental filtration applications [54]. The result herein obtained here indicates that the electrospraying of TiO_2 NPs did not significantly compromise pore interconnectivity or surface porosity. Overall, the combination of high porosity, controlled pore size distribution, and nanoscale surface functionalization suggests that the PAN/CA/TiO_2 NPs membrane is a promising candidate for applications requiring both mechanical breathability and selective barrier performance.

Table 5: Porosity parameters of PAN/CA/TiO_2 NPs membranes, including mean flow pore size (MFP), smallest and largest pore sizes, and total pore area percentage.

	PAN/CA/TiO_2 NPs
Bubble point pore size (µm)	15.530
MFP size (µm)	11.090
Smallest pore size (µm)	10.560
Total pore area (%)	54.71

3.4. Filtration Efficiency

Filtration efficiency is one of the most critical parameters in membrane performance. Higher filtration efficiency is often associated with thicker membranes, as increased thickness enhances the capture of particles within the fibrous network. However, a careful balance between maximizing filtration and keeping the membrane's breathability must be attended, since the latter is a critical factor in applications like air purification and facemasks. This balance is particularly significant for membranes functionalized with NPs, where surface modifications can further impact airflow and particle capture. The incorporation of TiO_2 NPs not only provides the membrane with antibacterial activity, but also contributes to particle retention through increased electrostatic interactions, which indirectly support long-term performance by preventing fouling and degradation. The uniform distribution of these NPs across the membrane surface leads to improved filtration performance.

In the filtration assays, polystyrene beads (Ø = 1 µm) were aerosolized through the sample port at a rate of 28.2 L/min and measured three times during 20 s for a total of 60 s. Table 6 shows the results of the filtration efficiency of PAN/CA/TiO_2 NPs membrane. The positive control showed a value of 11.07×10^5 particles during the

analysis. The PAN/CA/TiO_2 NPs membrane was tested in triplicate with the same conditions. The functionalized membranes demonstrated an average filtration efficiency of 82.3 %, showcasing their effectiveness in particulate removal. The performance is comparable to previous studies, where TiO_2-functionalized electrospun membranes typically exhibit filtration efficiencies in the range of 70–95% [55–58].

Table 6: Filtration efficiency of PAN/CA/ TiO_2 NPs membrane.

Sample	Number of Particles / 10^5	Filtration efficiency / %
Control	11.07 ± 0.32	
PAN/CA/TiO_2 NPs	1.96 ± 0.69	82.3 ± 6.2

When evaluated against CWA 17553:2020, the European Workshop Agreement for community face coverings, the filtration efficiency of 82.3% exceeds the minimum requirement of 70% for particles around 3 µm. Although the test in this study utilized smaller particles (1 µm), the results demonstrate that the membrane surpasses the standard for community face coverings, suggesting its potential to meet or exceed performance expectations for broader particle size ranges [59]. These findings suggest that the TiO_2-functionalized PAN/CA membranes show potential to be applied as an active filtration layer on community facemask prototypes.

3.5. Prototype development

With the aim of obtaining novel sustainable facemasks with enhanced active filtration ability, natural fiber-based woven fabric (cotton) was used as the outer layers of the facemask prototype, due to its good mechanical strength, low cost, biocompatibility, and breathability. The selected PAN/CA/TiO_2 NPs electrospun membrane was introduced as an inner layer. Facemask prototypes with one and two layers of the PAN/CA/TiO_2 NPs electrospun membrane were developed, as well as the control without the membrane (Figure 4).

Journal Pre-proof

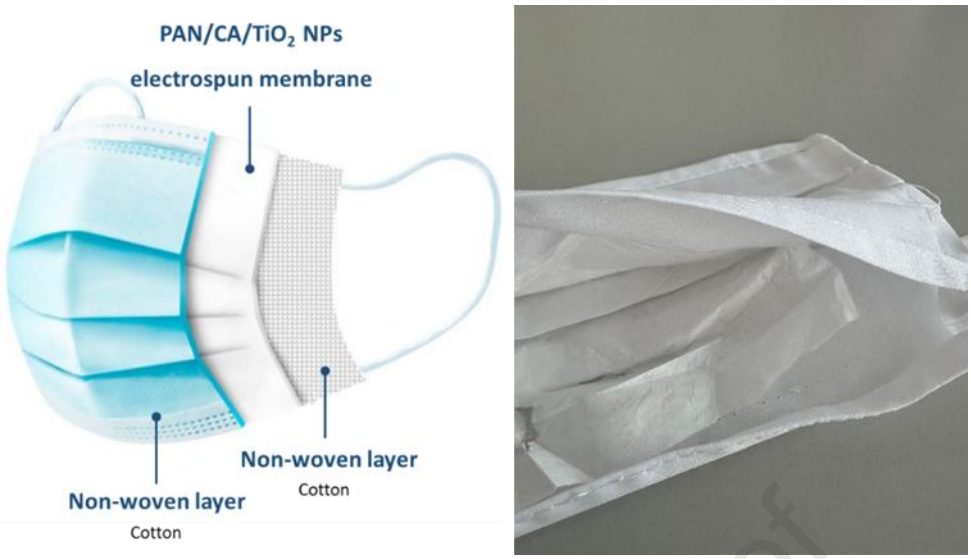


Figure 4: Schematic and photographic representation of facemask prototype comprising cotton outer layers and electrospun PAN/CA/TiO_2 NPs intermediate layer.

The air permeability of the facemask prototype was assessed and compared to the control (cotton + cotton prototype) and the PAN/CA/TiO_2 NPs electrospun membrane. The results are displayed in Table 7. The air permeability value obtained for PAN/CA electrospun membrane was 63.9 L/min. With the addition of TiO_2 NPs, a slight decrease in breathability is seen (52.3 L/min). Regarding the facemask prototypes, the control prototype (cotton + cotton) reveals a value of 34.4 L/min, while the introduction of one layer of the PAN/CA/TiO_2 NPs electrospun membrane does not decrease this value significantly (32.5 L/min). Furthermore, the introduction of two layers of the membrane results in a higher decrease in the air permeability (24.1 L/min); however, all values are significantly above the breathability reference value (8 L/min) [33,60]. These results correlate with the membranes' balance of filtration performance and breathability.

Table 7: Air permeability of PAN/CA membrane, PAN/CA/TiO_2 NPs membrane, control facemask prototype (cotton + cotton), facemask prototypes with 1 and 2 layers of PAN/CA/TiO_2 NPs membrane.

Sample	Air permeability (L/min)
PAN/CA	63.9 ± 5.1
PAN/CA/TiO_2 NPs	52.3 ± 5.2
Cotton + cotton	34.4 ± 5.8
Cotton + 1 layer PAN/CA/TiO_2 NPs + cotton	32.5 ± 9.6
Cotton + 2 layers PAN/CA/TiO_2 NPs + cotton	24.1 ± 5.8

Thermal management was also assessed for the facemask prototypes using a thermal camera recording the facial temperature in two different locations (nose and

mouth) during inhalation and exhalation. Images with no mask and with a surgical mask were also included for comparison. Figure 5 reveals the thermal images taken during inhalation and exhalation for the mentioned prototypes, and Table 8 shows the recorded facial temperatures.

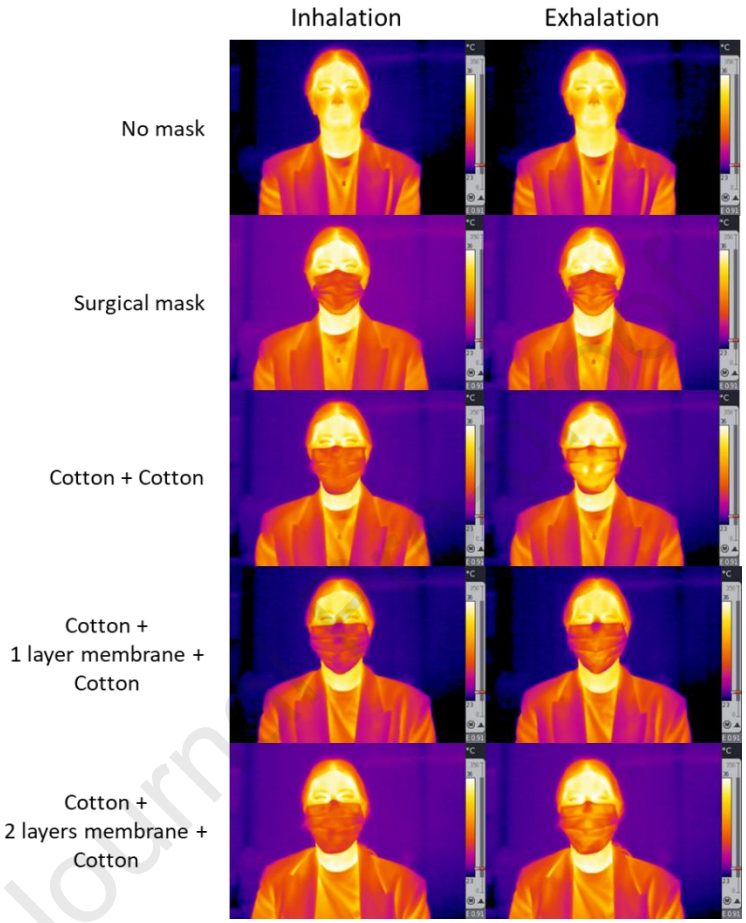


Figure 5: Thermal management images during inhalation and exhalation for a user wearing: no mask; a surgical mask; a control facemask prototype (cotton + cotton); facemask prototype with 1 layer of PAN/CA/TiO_2 NPs electrospun membrane; facemask prototype with 2 layers of PAN/CA/TiO_2 NPs electrospun membrane.

It can be seen that surgical masks reveal lower temperatures during inhalation (nose – 27.8 °C; mouth – 28.3 °C) and exhalation (nose – 28.0 °C; mouth – 28.8 °C). The control facemask prototype (cotton + cotton) reveals higher exhalation temperatures (nose – 32.4 °C; mouth – 33.4 °C). Regarding inhalation, the increase in the temperature is reduced, with the temperature values recorded close to the ones obtained for the surgical mask. The introduction of one and two layers of PAN/CA/TiO_2 NPs electrospun membrane shows no significant differences in the temperature values recorded during inhalation. The value recorded on the mouth zone for Cotton + 2 layers PAN/CA/TiO_2 NPs + Cotton during inhalation (27.8 °C) is even lower than the one obtained for the

surgical mask. Regarding the analysis during exhalation, both prototypes show temperature values higher than those obtained for the surgical mask. Nevertheless, the results are lower than the ones obtained for the control prototype, showing enhanced thermal comfort of these prototypes when compared with the Cotton + Cotton prototype.

Table 8: Recorded temperatures in two different zones (nose and mouth) during inhalation and exhalation for a user wearing: no mask; a surgical mask; a control facemask prototype (cotton + cotton); facemask prototype with 1 layer of PAN/CA/TiO_2 NPs electrospun membrane; facemask prototype with 2 layers of PAN/CA/TiO_2 NPs electrospun membrane.

	Temperature (°C)			
	Inhalation		Exhalation	
Type of membrane	**Nose**	**Mouth**	**Nose**	**Mouth**
Surgical mask	27.8	28.3	28.0	28.8
Cotton + Cotton	29.7	29.2	32.4	33.4
Cotton + 1 layer PAN/CA/TiO_2 NPs + cotton	28.7	28.3	29.7	31.7
Cotton + 2 layers PAN/CA/TiO_2 NPs + cotton	29.0	27.8	31.0	30.5

Journal Pre-proof

Journal Pre-proof

4. Conclusions

This work reports the development of PAN/CA membranes by electrospinning, followed by their surface functionalization with TiO_2 NPs by electrospraying, designed to act as active filtration layers in facemasks. Defect-free PAN and PAN/CA electrospun membranes were produced and characterized. The incorporation of 1% CA resulted in membranes with enhanced mechanical stability and a more homogeneous distribution of the fibers. Furthermore, ATR-FTIR analysis confirmed intermolecular interactions between PAN and CA.

TiO_2 NPs were successfully synthesized, revealing a spherical shape, high purity, and antibacterial activity against *Staphylococcus aureus* with a zone of inhibition halo between 15 and 15.5 mm. The functionalization of the membranes with TiO_2 NPs was carried out by electrospraying. GSDR and SEM/EDS analyses validated the presence of TiO_2 NPs on the surface of the PAN/CA/TiO_2 NPs electrosprayed membranes. TGA showed a 6.41% percentage of TiO_2 NPs in the PAN/CA membrane, while further confirming the chemical interactions between PAN and CA. WCA analysis showed no significant differences in membrane hydrophobicity following the TiO_2 deposition by electrospraying, while porosity analysis showed a mean pore size value of 11.09 µm and a total pore area of 54.71 %. These values, aligned with a narrow pore size distribution, indicate that the developed membrane falls into the ideal range for particulate filtration while maintaining effective air permeability.

Filtration assays using aerosolized polystyrene beads (Ø = 1 µm) revealed that the functionalized PAN/CA/TiO_2 membranes achieved an average filtration efficiency of 82.3%, demonstrating their strong potential for effective particulate removal and aligning with values typically reported for TiO_2-functionalized electrospun membranes. A balance between filtration efficiency and comfort properties is crucial for active filtration layers and, therefore, facemask prototypes were developed using two layers of cotton woven fabric as inner and outer layers, and PAN/CA/TiO_2 NPs membranes as intermediate layers. The prototypes were tested for air permeability, with all the facemask prototypes showing an air permeability value significantly above the breathability reference value (8 L/min). Thermal management was also assessed, showing suitable thermal comfort for the prototypes with the introduction of PAN/CA/TiO_2 NPs membrane layers.

Overall, the developed PAN/CA electrospun membranes, functionalized with TiO_2 NPs, show promise as intermediate layers in facemasks, enhancing user protection. The prototypes herein developed show adequate filtration efficiency (above the minimum requirement of 70% for particles around 3 μm, established by CWA 17553:2020) and microorganism degradation ability, while keeping compliance with standards for breathability and thermal comfort. To further evaluate the antimicrobial activity, a broader antimicrobial evaluation will be carried out for the final membranes including the TiO_2 NPs. Nevertheless, the facemask prototypes herein reported are ready-to-use prototypes that can be employed as community facemasks, complying with the required filtration standards for this type of mask.

From a socio-economic point of view, the development of electropspun PAN/CA membranes into facemasks is a cost-effective pathway to develop personal protective equipment complying with the standards. This approach is affordable (€0.05-€0.35/layer, considering the cost of reagents, solvents, consumables, and energy costs) while also compatible with scalable processes. The use of cotton woven fabric as outer layers and cellulose acetate for the composition of the electrospun layer will also lower the environmental impact of community facemasks, reducing the need for non-degradable plastics and mitigating waste management challenges associated with conventional masks.

Journal Pre-proof

Author Contributions

The manuscript was written through contributions of all authors. All authors have given approval to the final version of the manuscript. Conceptualization: RPCLS, JCA, SMC, DPF; Formal analysis: RPCLS, JCA, SMC, DPF; Funding acquisition: RF, DPF; Investigation: JMR, RPCLS, JCA, WA, VR; Project administration: RF, DPF; Supervision: RPCLS, DPF; Writing – original draft: JMR, RPCLS; Writing – review and editing: RPCLS, JCA, SMC, VR, DPF.

Acknowledgment

The authors acknowledge the financial support from the integrated project GIATEX—Gestão Inteligente da Água na ITV (Investment RE-C05-i01.01—Mobilizing Agendas/Alliances for Business Innovation), promoted by the Recovery and Resilience Plan (RRP), Next Generation EU, for the period 2022-2025, and from the European Regional Development Fund through the Operational Competitiveness Program. The authors also acknowledge the financial support from the National Foundation for Science and Technology of Portugal (FCT), under the projects UID/CTM/00264/2020 of the Centre for Textile Science and Technology (2C2T) on its components base (https://doi.org/10.54499/UIDB/00264/2020) and program (https://doi.org/10.54499/UIDP/00264/2020), and under the project DRI/India/0447/2020 (https://doi.org/10.54499/DRI/India/0447/2020).

Authors would like to express their gratitude to Dr. Dana Dutczak for the valuable assistance on porosity analysis.

References

1. Lyu, C.; Zhao, P.; Xie, J.; Dong, S.; Liu, J.; Rao, C.; Fu, J. Electrospinning of Nanofibrous Membrane and Its Applications in Air Filtration: A Review. *Nanomaterials* **2021**, *11*.

2. Wang, G.; Sun, L.; Zhao, B.; Fang, Y.; Qi, Y.; Ning, G.; Ye, J. Reusable Electrospun Nanofibrous Membranes with Antibacterial Activity for Air Filtration. *ACS Appl. Nano Mater.* **2023**, *6*, 10872–10880.

3. Zheng, G.; Shao, Z.; Chen, J.; Jiang, J.; Zhu, P.; Wang, X.; Li, W.; Liu, Y. Self-supporting three-dimensional electrospun nanofibrous membrane for highly efficient air filtration. *Nanomaterials* **2021**, *11*, 1–11.

4. Shim, E.; Jang, J. P.; Moon, J. J.; Kim, Y. Improvement of polytetrafluoroethylene membrane high-efficiency particulate air filter performance with melt-blown media. *Polymers (Basel).* **2021**, *13*.

5. Shao, Z.; Chen, Y.; Jiang, J.; Xiao, Y.; Kang, G.; Wang, X.; Li, W.; Zheng, G. Multistage-Split Ultrafine Fluffy Nanofibrous Membrane for High-Efficiency Antibacterial Air Filtration. *ACS Appl. Mater. Interfaces* **2022**, *14*, 18989–19001.

6. Naragund, V. S.; Panda, P. K. Electrospun nanofiber-based respiratory face masks—a review. *Emergent Mater.* **2022**, *5*, 261–278.

7. Ji, S. M.; Tiwari, A. P.; Oh, H. J.; Kim, H. Y. ZnO/Ag nanoparticles incorporated multifunctional parallel side by side nanofibers for air filtration with enhanced removing organic contaminants and antibacterial properties. *Colloids Surfaces A Physicochem. Eng. Asp.* **2021**, *621*, 126564.

8. Shao, W.; Niu, J.; Han, R.; Liu, S.; Wang, K.; Cao, Y.; Han, P.; Li, X.; Zhang, H.; Yu, H.; et al. Electrospun Multiscale Poly(lactic acid) Nanofiber Membranes with a Synergistic Antibacterial Effect for Air-Filtration Applications. *ACS Appl. Polym. Mater.* **2023**, *5*, 9632–9641.

9. Costa, S. M.; Pacheco, L.; Antunes, W.; Vieira, R.; Bem, N.; Teixeira, P.; Fangueiro, R.; Ferreira, D. P. Antibacterial and Biodegradable Electrospun Filtering Membranes for Facemasks: An Attempt to Reduce Disposable Masks Use. *Appl. Sci. 2022, Vol. 12, Page 67* **2021**, *12*, 67.

10. Haider, A.; Haider, S.; Kang, I. K. A comprehensive review summarizing the effect of electrospinning parameters and potential applications of nanofibers in biomedical and biotechnology. *Arab. J. Chem.* **2018**, *11*, 1165–1188.

11. Gong, X.; Yin, X.; Wang, F.; Liu, X.; Yu, J.; Zhang, S.; Ding, B. Electrospun Nanofibrous Membranes: A Versatile Medium for Waterproof and Breathable Application. *Small* **2023**, *19*, 2205067.

12. Li, X.; Wang, X. X.; Yue, T. T.; Xu, Y.; Zhao, M. L.; Yu, M.; Ramakrishna, S.; Long, Y. Z. Waterproof-breathable PTFE nano- and microfiber membrane as high efficiency PM2.5 filter. *Polymers (Basel).* **2019**, *11*, 1–14.

13. Roche, R.; Yalcinkaya, F. Electrospun Polyacrylonitrile Nanofibrous Membranes for Point-of-Use Water and Air Cleaning. *ChemistryOpen* **2019**, *8*, 97–103.

14. Nie, J.; Sun, B.; Jiao, T.; Liao, J.; Zhang, M.; Yang, R.; Li, Y. Biodegradable air filter with electrospun composite nanofibers and cellulose fibers dual network: Enhanced electrostatic adsorption, humidity resistance, and extended service life. *J. Hazard. Mater.* **2025**, *489*, 137557.

15. Zhu, X.; Kim, K. Electrospun polyacrylonitrile fibrous membrane for dust removal. *Front. Mater.* **2022**, *9*, 1–10.

16. Matulevicius, J.; Kliucininkas, L.; Prasauskas, T.; Buivydiene, D.; Martuzevicius, D. The comparative study of aerosol filtration by electrospun polyamide, polyvinyl acetate, polyacrylonitrile and cellulose acetate nanofiber media. *J. Aerosol Sci.* **2016**, *92*, 27–37.

17. Elaissaoui, I.; Sayeb, S.; Ounif, I.; Ferhi, M.; Karima, H. naifer; Ennigrou, D. J. Preparation and characterization of acetate cellulose electrospun nanofibers membrane: Potential application on wastewater treatment. *Heliyon* **2024**, *10*, e32552.

18. Nkabinde, S. C.; Moloto, M. J.; Matabola, K. P. Optimized Loading of TiO2 Nanoparticles into Electrospun Polyacrylonitrile and Cellulose Acetate Polymer Fibers. *J. Nanomater.* **2020**, *2020*.

19. Araújo, J. C.; Fangueiro, R. Protective Multifunctional Fibrous Systems Based on Natural Fibers and Metal Oxide Nanoparticles. **2021**, 1–25.

20. Wang, Z.; Pan, Z.; Wang, J.; Zhao, R. A Novel Hierarchical Structured Poly(lactic acid)/Titania Fibrous Membrane with Excellent Antibacterial Activity and Air Filtration Performance. *J. Nanomater.* **2016**, *2016*.

21. Orlando, R.; Polat, M.; Afshari, A.; Johnson, M. S.; Fojan, P. Electrospun Nanofibre Air Filters for Particles and Gaseous Pollutants. *Sustain.* **2021**, *13*, 1–18.

22. Pahasup-anan, T.; Suwannahong, K.; Dechapanya, W.; Rangkupan, R. Fabrication and photocatalytic activity of TiO2 composite membranes via simultaneous electrospinning and electrospraying process. *J. Environ. Sci. (China)* **2018**, *72*, 13–24.

23. Gumus, H. Catalytic performance of polyvinylidene fluoride (PVDF) supported TiO2 additive at microwave conditions. *J. Turkish Chem. Soc. Sect. A Chem.* **2020**, *7*, 361–374.

24. Kwon, M.; Kim, J.; Kim, J. Photocatalytic Activity and Filtration Performance of Hybrid TiO2-Cellulose Acetate Nanofibers for Air Filter Applications. *Polymers (Basel).* **2021**, *13*, 1–11.

25. Wen, Y.; Hu, Q.; Wang, X.; Zhang, W.; Chen, M. Electrospun Poly(m-phenyleneisophthalamide)/TiO2 Nanofiber Membranes for Particulate Matter Removal under High-Temperature Conditions. *ACS Appl. Polym. Mater.* **2024**, *6*, 1633–1644.

26. Kharaghani, D.; Kee Jo, Y.; Khan, M. Q.; Jeong, Y.; Cha, H. J.; Kim, I. S. Electrospun antibacterial polyacrylonitrile nanofiber membranes functionalized with silver nanoparticles by a facile wetting method. *Eur. Polym. J.* **2018**, *108*, 69–75.

27. Parekh, S. A.; David, R. N.; Bannuru, K. K. R.; Krishnaswamy, L.; Baji, A. Electrospun silver coated polyacrylonitrile membranes for water filtration applications. *Membranes (Basel).* **2018**, *8*, 26–29.

28. Maliszewska, I.; Czapka, T. Electrospun Polymer Nanofibers with Antimicrobial Activity. *Polymers (Basel).* **2022**, *14*, 1–32.

29. Chen, S.; Xie, Y.; Ma, K.; Wei, Z.; Ran, X.; Fu, X.; Zhang, C.; Zhao, C. Electrospun nanofibrous membranes meet antibacterial nanomaterials: From preparation strategies to biomedical applications. *Bioact. Mater.* **2024**, *42*, 478–518.

30. Feng, Q.; Wu, D.; Zhao, Y.; Wei, A.; Wei, Q.; Fong, H. Electrospun AOPAN/RC blend nanofiber membrane for efficient removal of heavy metal ions from water. *J. Hazard. Mater.* **2018**, *344*, 819–828.

31. Araújo, J. C.; Silva, P. M.; Cerqueira, M. A.; Teixeira, P.; Tira-Picos, V.; Neto, P.; Soares, O. S. G. P.; Graça, C. L.; Fangueiro, R.; Ferreira, D. P. Protective fibrous structures based on cellulose fibers functionalized with metal oxide nanoparticles by electrospinning and electrospray deposition. *Int. J. Biol. Macromol.* **2024**, *282*.

32. Ng, H. M.; Saidi, N. M.; Omar, F. S.; Ramesh, K.; Ramesh, S.; Bashir, S. Thermogravimetric Analysis of Polymers. *Encycl. Polym. Sci. Technol.* **2018**, 1–29.

33. International Organization of Standardization ISO 9237:1995. Textiles — Determination of the permeability of fabrics to air. 2017.

34. Kurokawa, N.; Kimura, S.; Hotta, A. Mechanical properties of poly(butylene succinate) composites with aligned cellulose-acetate nanofibers. *J. Appl. Polym. Sci.* **2018**, *135*, 1–9.

35. Wang, D.; Yue, Y.; Wang, Q.; Cheng, W.; Han, G. Preparation of cellulose acetate-

Journal Pre-proof

polyacrylonitrile composite nanofibers by multi-fluid mixing electrospinning method: Morphology, wettability, and mechanical properties. *Appl. Surf. Sci.* **2020**, *510*.

36. Jenab, A.; Roghanian, R.; Ghorbani, N.; Ghaedi, K.; Emtiazi, G. The efficacy of electrospun PAN/Kefiran nanofiber and kefir in mammalian cell culture: Promotion of PC12 cell growth, anti-MCF7 breast cancer cells activities, and cytokine production of PBMC. *Int. J. Nanomedicine* **2020**, *15*, 717–728.

37. Li, J.; Su, S.; Zhou, L.; Kundrát, V.; Abbot, A. M.; Mushtaq, F.; Ouyang, D.; James, D.; Roberts, D.; Ye, H. Carbon nanowalls grown by microwave plasma enhanced chemical vapor deposition during the carbonization of polyacrylonitrile fibers. *J. Appl. Phys.* **2013**, *113*.

38. Benavente, M. J.; Caballero, M. J. A.; Silvero, G.; López-Coca, I.; Escobar, V. G. Cellulose Acetate Recovery from Cigarette Butts. **2019**, 1447.

39. Buraso, W.; Lachom, V.; Siriya, P.; Laokul, P. Synthesis of TiO2 nanoparticles via a simple precipitation method and photocatalytic performance. *Mater. Res. Express* **2018**, *5*.

40. Raguram, T.; Rajni, K. S. Synthesis and analysing the structural, optical, morphological, photocatalytic and magnetic properties of TiO2 and doped (Ni and Cu) TiO2 nanoparticles by sol–gel technique. *Appl. Phys. A Mater. Sci. Process.* **2019**, *125*, 1–11.

41. Khashan, K. S.; Sulaiman, G. M.; Abdulameer, F. A.; Albukhaty, S.; Ibrahem, M. A.; Al-Muhimeed, T.; Alobaid, A. A. Antibacterial Activity of TiO2 Nanoparticles Prepared by One-Step Laser Ablation in Liquid. *Appl. Sci.* **2021**, *11*.

42. Pant, B.; Park, M.; Park, S. J. Recent advances in TiO2 films Prepared by Sol-gel Methods for Photocatalytic Degradation of Organic Pollutants and Antibacterial Activities. *Coatings* **2019**, *9*, 1–19.

43. Huang, K.; Chen, L.; Liao, M.; Xiong, J. The photocatalytic inactivation effect of Fe-doped TiO2 nanocomposites on leukemic HL60 cells-based photodynamic therapy. *Int. J. Photoenergy* **2012**, *2012*.

44. Bazgir, S. Preparation and Characterization of Carbon Nanofibers via Electrospun PAN Nanofibers. **2009**, *3*.

45. Xue, T. J.; McKinney, M. A.; Wilkie, C. A. The thermal degradation of polyacrylonitrile. *Polym. Degrad. Stab.* **1997**, *58*, 193–202.

46. Li, J.; Zhang, L. P.; Peng, F.; Bian, J.; Yuan, T. Q.; Xu, F.; Sun, R. C. Microwave-Assisted Solvent-Free Acetylation of Cellulose with Acetic Anhydride in the Presence of Iodine as a Catalyst. *Molecules* **2009**, *14*, 3551–3566.

47. Lin, Z.; Wang, Z.; Zhang, X.; Diao, D. Superhydrophobic, photo-sterilize, and reusable mask based on graphene nanosheet-embedded carbon (GNEC) film. *Nano Res.* **2021**, *14*, 1110–1115.

48. Boinovich, L. B.; Emelyanenko, A. M. Hydrophobic materials and coatings: principles of design, properties and applications. *Russ. Chem. Rev.* **2008**, *77*, 583–600.

49. Jung, B.; Yoon, J. K.; Kim, B.; Rhee, H. W. Effect of crystallization and annealing on polyacrylonitrile membranes for ultrafiltration. *J. Memb. Sci.* **2005**, *246*, 67–76.

50. Du, C.; Wang, Z.; Liu, G.; Wang, W.; Yu, D. One-step electrospinning PVDF/PVP-TiO2 hydrophilic nanofiber membrane with strong oil-water separation and anti-fouling property. *Colloids Surfaces A Physicochem. Eng. Asp.* **2021**, *624*, 126790.

51. Pais, V.; Navarro, M.; Guise, C.; Martins, R.; Fangueiro, R. Hydrophobic performance of electrospun fibers functionalized with TiO2 nanoparticles. *Text. Res. J.* **2022**, *92*, 2719–2730.

52. Thota, K.; Araga, R.; Sabapathy, M.; Kakunuri, M. Polystyrene Nanofibrous Membrane Infused with TiO2 Nanoparticles by a One-Step Electrospinning Process for Effective Oil-Water Separation. *Ind. Eng. Chem. Res.* **2024**, *63*, 14249–14258.

53. Naragund, V. S.; Panda, P. K. Electrospun polyacrylonitrile nanofiber membranes for air filtration application. *Int. J. Environ. Sci. Technol.* **2022**, *19*, 10233–10244.

54. Ul, W.; Kim, M.; Choi, J.; Yoo, K.; Kurniawan, R.; Jo, T. Optimization of porosity and tensile strength of electrospun polyacrylonitrile nanofibrous membranes. *Mater. Chem. Phys.* **2019**, *229*, 310–318.

55. Hartati, S.; Zul, A.; Yuniar, P.; Maulida, D.; Yudhowijoyo, A.; Dioktyanto, M.; Saputro, K. E.; Tau, N. Synthesis of Electrospun PAN/TiO2/Ag Nanofibers Membrane As Potential Air Filtration Media with Photocatalytic Activity. **2022**.

56. Su, J.; Yang, G.; Cheng, C.; Huang, C.; Xu, H.; Ke, Q. Hierarchically structured TiO2/ PAN nanofibrous membranes for high-efficiency air filtration and toluene degradation. *J. Colloid Interface Sci.* **2017**, *507*, 386–396.

57. Lin, M.; Shen, J.; Qian, Q.; Li, T.; Zhang, C.; Qi, H. Fabrication of Poly (Lactic Acid) @TiO2 Electrospun Membrane Decorated with Metal – Organic Frameworks for Efficient Air Filtration and Bacteriostasis. **2024**.

58. Orlando, R.; Gao, Y.; Fojan, P.; Mo, J. Filtration Performance of Ultrathin Electrospun Cellulose Acetate Filters Doped with TiO2 and Activated Charcoal. *Buildings* **2021**, *11*, 1–15.

59. European Committee for Standardization *CWA 17553:2020 - Community face coverings: Guide to minimum requirements, methods of testing, and use*; 2020.

60. INFARMED – Autoridade Nacional do Medicamento e Produtos de Saúde, I. . . Masks for use in COVID-19 – Technical specificities.

Journal Pre-proof

Journal Pre-proof

PAN/CA-based electrospun membranes for air filtration and active microorganism degradation

Joana M. Rocha [1], Rui P. C. L. Sousa [1,*], Joana C. Araújo [1], Sofia M. Costa [1], Wilson Antunes [2], Verónica Rocha [1], Raul Fangueiro [1], and Diana P. Ferreira [1,*]

[1] Centre for Textile Science and Technology (2C2T), University of Minho, 4800-056 Guimarães, Portugal

[2] Centro de Investigação da Academia Militar (CINAMIL), Unidade Militar Laboratorial de Defesa Biológica e Química (UMLDBQ, Instituto Universitário Militar), Av. Dr. Alfredo Bensaúde, 1849-012 Lisboa, Portugal

Correspondence: rui.sousa@2c2t.uminho.pt; diana.ferreira@det.uminho.pt

Highlights:

- Polyacrylonitrile (PAN) and cellulose acetate (CA) were combined to develop an electrospun membrane.
- Electrospraying was used to functionalize the membrane with titanium dioxide (TiO2) nanoparticles (NPs).
- PAN/CA/TiO_2 NPs membranes showed filtration efficiency above 80% for 1 µm particles.
- Facemask prototypes were developed using cotton and PAN/CA/TiO_2 NPs layers.
- Air permeability and thermal imaging endorsed the comfort properties of the prototypes.

Journal Pre-proof

Journal Pre-proof

Declaration of interests

☒ The authors declare that they have no known competing financial interests or personal relationships that could have appeared to influence the work reported in this paper.

☐ The authors declare the following financial interests/personal relationships which may be considered as potential competing interests:

Journal Pre-proof